33RD INTERNATIONAL COSMIC RAY CONFERENCE, RIO DE JANEIRO 2013
THE ASTROPARTICLE PHYSICS CONFERENCE

Atmospheric neutrinos at high energy

EUN-JOO AHN[1], RALPH ENGEL[2], ANATOLI FEDYNITCH[2,3], THOMAS K. GAISSER[4], FELIX RIEHN[2,4], TODOR STANEV[4].

[1] *Center for Particle Astrophysics, Fermi National Accelerator Laboratory, Batavia, IL 60510-0500, USA*
[2] *Karlsruher Institut für Technologie, Institut für Kernphysik, Postfach 3640, 76021 Karlsruhe, Germany*
[3] *CERN, CH-1211 Geneva 23, Switzerland*
[4] *Bartol Research Institute, Department for Physics and Astronomy, University of Delaware, Newark, DE 19716, USA*

Email of contact person

Abstract: Finding neutrinos of astrophysical origin requires a good understanding of the flux of atmospheric neutrinos up to the PeV energy range. Of particular importance is the level of prompt leptons, and the effect of the knee in the primary spectrum of nucleons. In this paper we describe techniques for combining Monte Carlo simulations with analytic approximations to overcome the technical problem of low statistics in the Monte Carlo. We will present preliminary results of our calculations based on the latest version of the SIBYLL event generator with charm.

Keywords: Atmospheric neutrinos, primary cosmic ray flux, hadron interaction models, charm production, LHC

1 Introduction

The spectrum of atmospheric leptons is a convolution of the primary spectrum of cosmic-ray nucleons with the production of mesons and their decay products in the resulting cascade. Simple analytic approximations [1, 2] assume scaling and power-law primary spectra. In reality, the spectrum is not described by a single power over a large energy range, and the fractional energy of secondary hadrons also evolves with energy. The most straightforward approach to account for these effects is to use a Monte Carlo calculation in which the yields of leptons are calculated as a function of primary energy per nucleon. The lepton spectra can then be composed for an arbitrary primary spectrum. This approach is limited at the highest energies by statistical uncertainties in the Monte Carlo simulation due to the low decay probability of pions and kaons at high energy.

There are at least two ways to obtain numerical results with no statistical uncertainties. One is to follow the method of Thunman, Ingelmann and Gondolo (TIG-96)[3] in which the analytic forms of the cascade equations are modified by defining energy-dependent Z-factors (spectrum weighted moments of the production and decay distributions) that account both for the violation of scaling in hadron production and for the deviation of the primary spectrum fom a power law. Another approach following Bossard et al. [4] is to carry out a stepwise integration of the integro-differential cascade equations starting from the incident spectrum of nucleons. We adopt the latter approach here.

Major sources of uncertainty in the lepton spectra in the 100 TeV range and above come from uncertain knowledge of charm production and from iuncertainties in the primary spectrum itself. In this paper we comment on the primary spectrum first. We then describe how production of charm is treated in a new version of the event generator Sibyll2.2f [7] that is currently under construction. Results are illustrated by comparing lepton fluxes for various assumptions about the shape and elemental composition of the primary spectrum.

2 Parametrization of inclusive nucleon flux

To illustrate the level of uncertainty in the primary spectrum of nucleons, we show in Figure 1 several fits based on air shower measurements of the all-particle spectrum together with assumptions about the energy dependence of the composition. The Polygonato model [8] is shown with its Galactic component only. Three fits labelled GST 3-gen, GST 4-gen and H3a are described in a recent paper [9]. For later reference, we also show the nucleon spectrum that has been used for calculations of charm production in the atmosphere [3, 10].

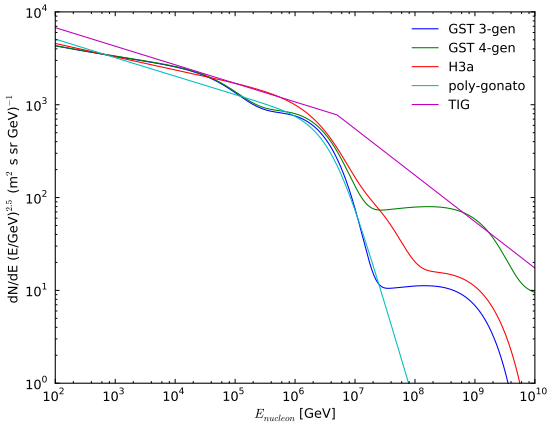

Figure 1: Comparison of parametrizations of the inclusive nucleon flux up to very high energy.

All the models show the effect of the knee in the cosmic-ray spectrum. The manifestation of the knee in the specturm of nucleons depends significantly on the primary composition because heavy nuclei contribute relatively much more at a given energy per particle than to the spectrum of nucleons. Because of the steep spectrum, the contribution of a nucleus of mass A is suppressed by a factor of $(1/A)^{\gamma}$, where $\gamma \sim 1.7$. The models based on air shower measure-

ments in the PeV region and above all show a significantly lower energy for the knee in the nucleon spectrum than was assumed in the calculations of the charm contribution to the lepton fluxes in Refs. [3, 10]).

3 Charm production in the SIBYLL model

Because of the large mass of the charmed quark, charm production can be calculated in the context of perturbative QCD, as in the calcultions of Refs. [3] and [10]. In fact, however, experiments show charm production at energies as low as $\sqrt{s} = 20\,\text{GeV}$ at a level higher than would be expected given the mass of the charmed quark if perturbative QCD accounted for all production. Moreover, certain features such as the dominance of charmed hyperon production over its anti-particle [11] also sugest some contriubtion of non-perturbative effects in the production of charm.

The event generator SIBYLL lends itself to a consistent description of charm that includes both perturbative and non-perturbative components. Production of secondary particles in this model is accomplished by the fragmentation of strings or color flux tubes which are stretched in energy and split to hadronize by production of $q\bar{q}$ (or di-quark, anti-di-quark) pairs. The same splitting occurs when pairs of strings are stretched between valence constituents in the two colliding hadrons (non-perturbative) or when a string is stretched between pairs of partons emerging from a hard (perturbative QCD) scattering of partons from the incident hadrons. To describe it another way, the non-perturbative mechanism is represented by charm production in the fragmentation of valence quark-valence/sea-quark strings and diffractive strings. The perturbative contribution is assumed to be proportional to the inclusive minijet cross section and is implemented as charm production in the fragmentation of strings attached to minjets.

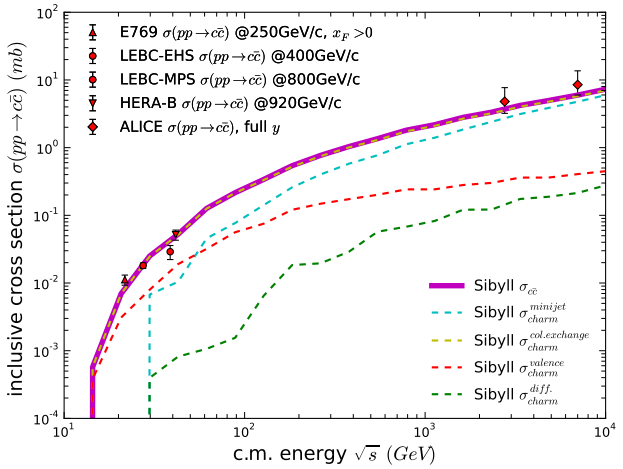

Figure 2: Comparison of inclusive charm production cross section with a compilation of acclerator data [14, 15, 16, 17, 18, 19].

Figure 2 gives a global overview of how the two components add up to give the total charm production cross section. The non-perturbative contribution dominates the total production cross section at low energy, while the mini-jet contribution dominates at high energy. The non-perturbative production may exhibit some of the features of models with intrinsic charm [12, 13] because of the association with the

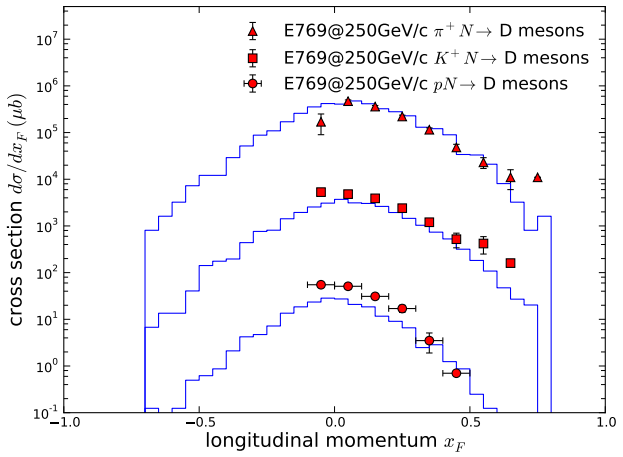

Figure 3: Example illustrating the description of charm production at fixed-target experiments [16].

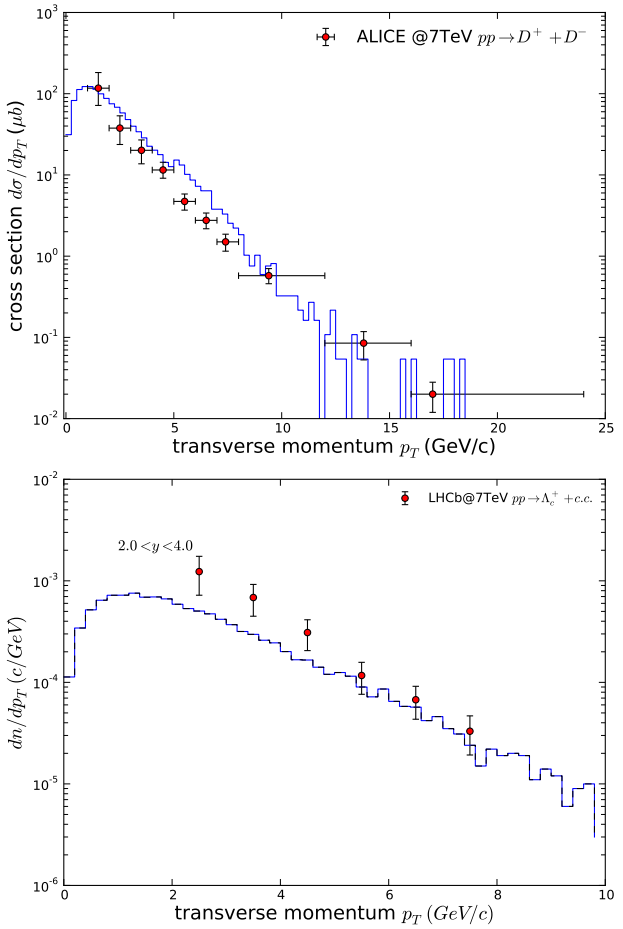

Figure 4: Examples illustrating the description of charm production at LHC [14, 20].

projectile momentum. The perturbative (mini-jet) component has similar kinematics to production in conventional QCD calculations of charm production.

Since each experiment in fact measures charm production at a particular energy and in a limited region of phase space, it is important that the parameters of the model be adjusted to each individual measurement in a way that maintains consistency with production of pions and kaons and traces

the observed energy dependence of production of all particle flavors. Because it maintains energy and flavor conservation, Sibyll offers a suitable framework for adding production of charm in a consistent manner. Fig. 3 is an example of a fit to fixed target date, while Fig. 4 illustrates how the model fits measurements of charm production at LHC.

4 Matrix method for calculating lepton fluxes

Following Lipari [2], we write the equation for the evolution of the flux of hadrons of type h in the atmosphere for one energy bin E_i as

$$\begin{aligned}\frac{\mathrm{d}\phi_h(E_i)}{\mathrm{d}X} &= \\ &- \frac{\phi_h(E_i)}{\lambda_{int}^{(h)}(E_i)} + \sum_{E_k \geq E_i} \sum_k \frac{c_{k\to h}(E_i,E_k)}{\lambda_{int}^{(k)}(E_k)} \phi_k(E_k) \\ &- \frac{\phi_h(E_i)}{\lambda_{dec}^{(h)}(E_i,X)} + \sum_{E_k \geq E_i} \sum_k \frac{d_{k\to h}(E_i,E_k)}{\lambda_{dec}^{(k)}(E_k,X)} \phi_k(E_k).\end{aligned} \quad (1)$$

The interaction length in air $\lambda_{int}^{(h)}(E_i) = m_{Air}/\sigma_{hA}^{inel}(E_i)$ is calculated using the SIBYLL-2.2F or QGSJET-01C cross-sections. The decay length of hadrons in air $\lambda_{dec}^{(h)}(E_i,X) = \frac{c\tau_h E_i \rho_{Air}(X)}{m_h c^2}$ [1] is parametrized using an exponential representation of the US Standard atmosphere [21] from the CORSIKA air shower simulation [22]. The columns of the matrices **C** and **D** contain the inclusive energy spectra obtained through sampling of the Monte-Carlo interaction models SIBYLL-2.2 and QGSJET-01C. The matrix element $c_{p\to\pi^+}$ divided by the interaction length of the mother meson, i.e.

$$\frac{c_{p\to\pi^+}(E_i,E_k)}{\lambda_{int}^{(p)}(E_k)}, \quad (2)$$

gives the rate at which protons at lab energy E_k are converted into pions with energy $E_i < E_k$ during the cascade evolution as a function of the atmospheric depth X.

The equations for leptons have the same form as Eq. 1, except that the interaction terms are neglected and leptons are exclusively produced through decays of mesons and baryons.

To solve this system of equations we perform a numerical integration similar to that used in Ref. [4, 5, 6] that steps through the atmosphere along the direction of the primary particle incrementing the particles of each type that arise from interactions and decays of particles present in the previous step. The integration starts from the primary spectrum of nucleons at the top of the atmosphere. The numerical integration is set up in matrix form so that a standard integrator can be used to perform the numerical integration of the coupled cascade equations.

We now rewrite this coupled system of ordinary differential equations into an algebraic form. Using the notation

$$\vec{\phi} = \begin{pmatrix} \phi_p(E_0) \\ \phi_p(E_1) \\ \cdots \\ \phi_p(E_N) \\ \phi_n(E_0) \\ \cdots \\ \phi_n(E_N) \\ \phi_\pi^+(E_0) \\ \cdots \\ \phi_{\bar{\nu}_e}(E_N) \end{pmatrix}, \quad (3)$$

$$C_{p\to p} = \begin{vmatrix} c_{p\to p}(E_0,E_0) & \cdots & c_{p\to p}(E_0,E_N) \\ 0 & \ddots & c_{p\to p}(E_1,E_N) \\ 0 & \cdots & c_{p\to p}(E_N,E_N) \end{vmatrix}, \quad (4)$$

the quadratic interaction matrix **C** is constructed by arranging the sub-matrices $C_{k\to h}$ according to the state vector $\vec{\phi}$ (Eq. 3)

The decay matrix **D** is constructed in a similar way using inclusive decay spectra obtained from sampling the PYTHIA 8 [23] event generator. The hadrons $p, n, \pi^+, \pi^-, K^+, K^-, K_L^0, K_S^0, D^0, D^-, D^+$ and the leptons $\mu^+, \mu^-, \nu_\mu, \bar{\nu}_\mu, \nu_e, \bar{\nu}_e$ are explicitly treated in this method. The matrices $\bar{\Lambda}_{int}^{(h)}$ and $\bar{\Lambda}_{dec}^{(h)}$ contain the reciprocal interaction and decay lengths on the diagonal elements. Comparing with equation one, we can now write the cascade equations in matrix form as:

$$\frac{\mathrm{d}\vec{\phi}}{\mathrm{d}X} = \left[(-\mathbb{1}+\mathbf{C})\bar{\Lambda}_{int} + (-\mathbb{1}+D)\bar{\Lambda}_{dec}(X)\right]\vec{\phi}. \quad (5)$$

For physical conditions, i.e. $\vec{\phi}(X) \geq 0$, all eigenvalues are < 0, the solution of this system of ordinary differential equations can be found numerically by integration of

$$\vec{\phi}(X) = \exp\left(\left[(-\mathbb{1}+\mathbf{C})\bar{\Lambda}_{int} + (-\mathbb{1}+\mathbf{D})\bar{\Lambda}_{dec}(X)\right]X\right)\vec{\phi}_0(X_0).$$

The nuclei are treated in the superposition approach, which we assume to approximately hold for average inclusive spectra of atmospheric leptons.

5 Results and discussion

The results of our calculations of lepton fluxes are shown as solid black lines in Fig. 5. The plots include conventional leptons from decay of pions and kaons, which dominate at low energy and prompt leptons from decay of charm, which dominate at high energy. Muons (sum of both charges) are highest, $\nu_\mu + \bar{\nu}_\mu$ are lower and $\nu_e + \bar{\nu}_e$ the lowest. Dashed black lines trace the conventional component of each flavor and dotted black lines the prompt component. The crossover occurs at $\sim$ 30 TeV for electron neutrinos, just below 1 PeV for muon neutrinos and around 2 PeV for muons. Also shown in red are the results from charm version of QGSJET [24] and points from the corresponding Monte Carlo calculation from Ref. [25]. Charm in Sibyll2.2f is about a factor of five higher than in QGSjet.

These fluxes are compared with the charm fluxes of TIG-96 [3] (thin orange line) and with the more recent charm calculation of Enberg, Sarcevic & Reno (ERS) [10] (grey band). For these two calculations, only the charm contribution to the flux of $\mu^+ + \mu^-$ is shown. (The charm

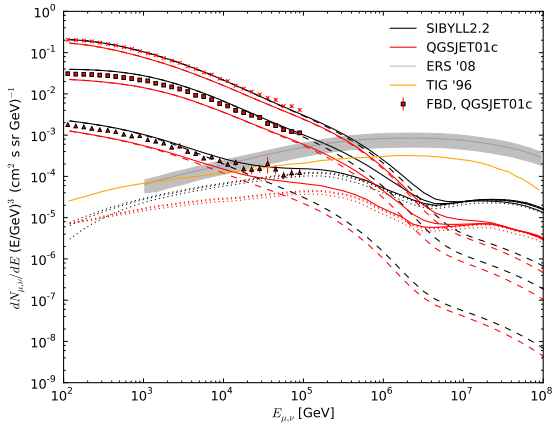

Figure 5: Comparison of results of this work with previously published fluxes.

contribution to $\nu_\mu + \bar{\nu}_\mu$ and to $\nu_e + \bar{\nu}_e$ is approximately equal). The prompt lepton fluxes of the present calculation with Sibyll2.2f are more than an order of magnitude lower than TIG-96 and ERS at energies $> 10^6$ GeV. This is mainly a consequence of our more realistic treatment of the knee in the parent nucleon spectrum.

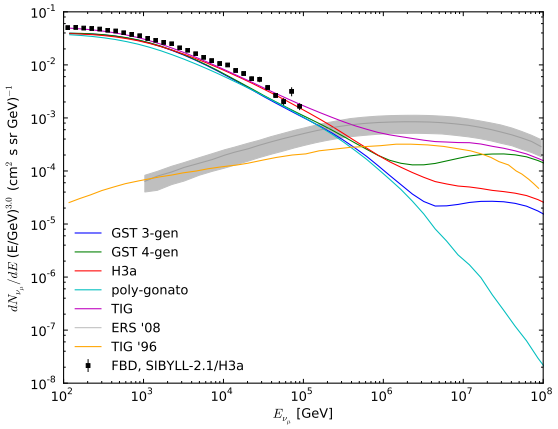

Figure 6: Illustration of importance of primary flux for inclusive lepton fluxes at very high energy.

Further qualitative conclusions about uncertainties in prompt leptons can be inferred from Fig. 6, which shows the spectrum of $\nu_\mu + \bar{\nu}_\mu$ from Sibyll2.2f calculated with five different assumptions for the primary spectrum of nucleons. It is interesting that when we use the TIG primary spectrum, we get a level of prompt neutrinos that is between that of TIG and ERS. In the important region arount $E_\nu \sim 1$ PeV, the predictions of the more realistic models span a range of about a factor of two in flux. This indicates the level of uncertainty in the neutrino flux due to uncertainties in the primary spectrum.

References

[1] T.K. Gaisser, *Cosmic Rays and Particle Physics*, (Cambridge University Press, 1990).
[2] P. Lipari, Astropart. Phys. 1 (1993) 195–227.
[3] M. Thunman, G. Ingelman, and P. Gondolo, Astropart. Phys. 5 (1996) 309–332.
[4] G. Bossard, H. Drescher, N. Kalmykov, S. Ostapchenko, A. Pavlov, T. Pierog, E. Vishnevskaya, and K. Werner, Phys. Rev. D63, 054030 (2001).
[5] J. Drescher and G. Farrar, Physical Review D67, 116001.
[6] T. Bergmann et al., Astropart. Phys. 26 (2007) 420-432.
[7] E. J. Ahn et al., these proceedings, id 0803.
[8] J. Hörandel, Astropart. Phys. 19 (2003) 193–220.
[9] T. Gaisser, T. Stanev, and S. Tilav, arXiv:1305.3565 (2013) .
[10] R. Enberg, G. Ingelman, and P. Gondolo, Phys. Rev. D78 (2008) 043005.
[11] S. Collaboration, Phys. Lett. B 528 (2002) 49.
[12] S.J. Brodsky et al., Phys. Lett. B 93 (1980) 451.
[13] E.V. Bugaev et al., Nuovo Cimento C12 (1989) 41.
[14] B. Abelev *et al.* (ALICE Collaboration Collab.), JHEP 1201 (2012) 128 and arXiv:1111.1553 [hep-ex].
[15] B. Abelev *et al.* (ALICE Collaboration Collab.), JHEP 1207 (2012) 191 and arXiv:1205.4007 [hep-ex].
[16] G. A. Alves *et al.* (E769 Collaboration Collab.), Phys.Rev.Lett. 77 (1996) 2392–2395.
[17] M. Aguilar-Benitez *et al.* (LEBC-EHS Collaboration Collab.), Z.Phys. C40 (1988) 321.
[18] R. Ammar, R. C. Ball, S. Banerjee, P. C. Bhat, P. Bosetti, *et al.*, Phys.Rev.Lett. 61 (1988) 2185–2188.
[19] A. Zoccoli *et al.* (HERA-B Collaboration Collab.), Eur.Phys.J. C43 (2005) 179–186.
[20] R. Aaij *et al.* (LHCb collaboration Collab.), Nucl.Phys. B871 (2013) 1–20 and arXiv:1302.2864 [hep-ex].
[21] *Standard Atmosphere*, U.S. Government Printing Office, 1976).
[22] D. Heck, J. Knapp, J. Capdevielle, G. Schatz and T. Thouw, Report No. FZKA 6019, 1998 (unpublished).
[23] T. Sjöstrand, S. Mrenna and P. Skands, JHEP (2006) 026.
[24] S. Ostapchenko, Nucl. Phys. B Proc. Suppl, 151 (2006) 143V146.
[25] A. Fedynitch, J. Becker Tjus & P. Desiati, P. Phys. Rev. D86 (2012) 114024.